

ORIGINAL ARTICLE

Nontargeted urine metabolomic analysis of acute intermittent porphyria reveals novel interactions between bile acids and heme metabolism: New promising biomarkers for the long-term management of patients

Thibaud Lefebvre^{1,2,3,4}  | Thibaut Eguether⁵ | Etienne Thévenot⁴ |
Antoine Poli^{1,2,3,4} | Emeline Chu-Van⁴ | Pranvera Krasniqi⁵ |
Caroline Schmitt^{1,2,3} | Neila Talbi^{1,2,3} | Gaël Nicolas^{1,3} | Hervé Puy^{1,2,3} |
Christophe Junot⁴ | Antonin Lamazière⁵ | Florence Castelli⁴ |
Laurent Gouya^{1,2,3}  | François Fenaille⁴

¹Université Paris Cité, INSERM U1149, Centre de Recherche sur l'Inflammation, Paris, France

²Assistance Publique-Hôpitaux de Paris, Centre de Référence Maladies Rares Porphyries, Hôpital Louis Mourier, Colombes, France

³Laboratory of Excellence Gr-Ex, Paris, France

⁴Université Paris-Saclay, CEA, INRAE, Département Médicaments et Technologies pour La Santé (DMTS), MetaboHUB, Gif-sur-Yvette, France

⁵Sorbonne Université, INSERM, AP-HP, Centre de Recherche Saint-Antoine, CRSA, Paris, France

Correspondence

Laurent Gouya, CRMR Porphyrie, Hôpital Louis Mourier, 178 rue des Renouillers, 92701 Colombes Cedex, France.
Email: laurent.gouya@inserm.fr

Funding information

Assistance Publique-Hôpitaux de Paris

Communicating Editor: Georg Hoffmann

Abstract

Acute intermittent porphyria is an inherited error of heme synthesis. The underlying pathophysiology, involving mainly hepatic heme synthesis, is poorly understood despite its occurrence, and the severity of acute porphyria attack is still difficult to control. A better understanding of the interactions between heme synthesis and global metabolism would improve the management of AIP patients. An untargeted metabolomic analysis was performed on the urine of 114 patients with overt AIP and asymptomatic carriers using liquid chromatography coupled to high-resolution mass spectrometry. The collected data were analyzed by combining univariate and multivariate analyses. A total of 239 metabolites were annotated in urine samples by matching chromatographic and mass spectral characteristics with those from our chemical library. Twenty-six metabolites, including porphyrin precursors, intermediates of tryptophan or glycine metabolism and, unexpectedly, bile acids, showed significant concentration differences between the phenotypic groups. Dysregulation of bile acid metabolism was confirmed by targeted quantitative analysis, which revealed an imbalance in favor of hydrophobic bile acids associated with changes in conjugation, which was more pronounced in the severe phenotype. Using a random forest model, the cholic acid/chenodeoxycholic acid ratio enables the differential classification of severe patients from other patients with a diagnostic accuracy of 84%. The analysis of urine samples revealed

significant modifications in the metabolome of AIP patients. Alteration in bile acids provides new insights into the pathophysiology of chronic complications, such as primary liver cancer, while also providing new biomarker candidates for predicting the most severe phenotypes.

KEYWORDS

acute hepatic porphyria, bile acid, chenodeoxy, cholic acid, heme, high resolution mass spectrometry

1 | INTRODUCTION

Acute intermittent porphyria (AIP) is an autosomal dominant disorder caused by a defect in the third enzyme of the heme biosynthesis pathway, hydroxymethylbilane synthase (HMBS), which is encoded by the *HMBS* gene. HMBS defects lead to a metabolic bottleneck, which is responsible for the accumulation of delta-aminolevulinic acid (ALA) and porphobilinogen (PBG). These metabolites mainly produced by the liver are associated with the onset of neurological symptoms: the acute porphyria attacks (APA). APA is characterized by severe abdominal pain, dysautonomic symptoms, and peripheral and central neurological symptoms.¹ In the liver, heme biosynthesis is inducible. Thus a partial HMBS enzyme defects become apparent when heme requirements increase, due to the induction of the first enzyme, ALA synthase-1 (ALAS-1) at the transcriptional, translational and post-translational levels.² AIP is a rare disease with an estimated prevalence of patient with current and past symptoms of 5.9 per million in Europe.³ However *HMBS* mutations have an estimated prevalence far higher, ranging between 1/1786 and 1/1299, depending on the calculation method.^{4,5} *HMBS* mutation carriers are considered to be overt patients if at least one APA was diagnosed based on clinical and biological criteria. Most patients suffer from one to a few attacks during their whole life, but between 3% and 8% of patients present with recurrent acute attacks at least four times per year.^{3,6} Furthermore, the penetrance of *HMBS* variants is less than 1% in the general population and the expressivity is extremely variable and unpredictable, suggesting the existence of additional genetic or environmental factors modulating the phenotype which are not yet fully understood. Preventive measures for APA, such as avoiding porphyrinogenic drugs, are highly restrictive and are applied indiscriminately to all patients, whereas only a minority of patients present with acute symptoms.⁷ Recently, an innovative treatment based on a small interfering RNA that inhibits ALAS1 and specifically targets the liver has been commercialized, with remarkable efficacy in reducing the number of APA.⁸

Heme, porphyrins, and precursors, ALA and PBG, are closely linked to intermediary metabolism since ALA synthesis results from the condensation of succinyl-CoA and glycine, two of its key metabolites. In addition, the final heme product is a cofactor of many important metabolic enzymes and consequently has a major role in liver metabolism.^{9–11} Perturbations in other metabolic pathways have been previously reported in acute porphyria (AP), such as imbalance between tryptophan and kynurenine in tryptophan metabolism, increased homocysteine levels, mitochondrial energetic failure or modified glycine concentrations in recurrent patients.^{11–16} Most of the metabolic investigations in humans were performed on blood using targeted tandem mass spectrometry coupled with liquid chromatography (LC–MS/MS).^{15–17} One untargeted approach involving NMR analysis in urine was reported.¹³ Urine is recognized as the preferred fluid in AP management. This is due to the ease of collecting and shipping urine samples, but above all to the historical quantification of urinary ALA and PBG, the acute attack biomarkers. Now, sensitive LC–MS approaches enable their quantification in blood.¹⁸

The aim of this study was to explore, without any a priori assumptions, the difference in urinary metabolic profiles between asymptomatic carriers and overt patients presenting with mild and severe phenotypes. Our goal was to identify new biomarker candidates that would help predicting disease onset, progression to recurrence and potential comorbidities severity while also better delineating the underlying pathophysiological mechanisms triggering an acute attack.

2 | MATERIALS AND METHODS

2.1 | Study design

The study design is summarized in Figure 1. For untargeted metabolomics, a first panel of 114 urine samples was collected from either patients with overt disease or patient with latent porphyria (LP) followed by the French Center for Porphyria (Table S1). Specifically defined for

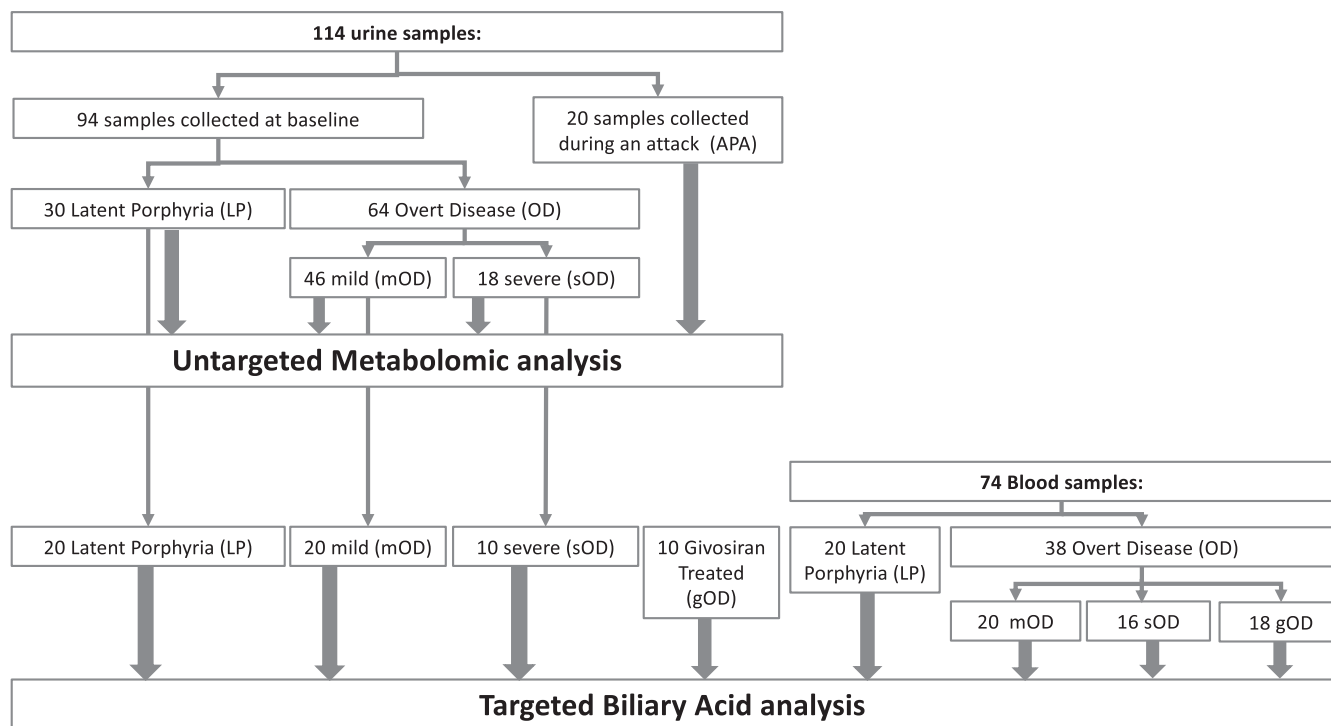


FIGURE 1 Summary of all samples used for the untargeted and targeted analyses.

this study because the number of patients in “active acute porphyria” defined by Stein et al. is too restrictive,¹⁹ overt disease refers to carriers of an *HMBS* deleterious variant who experienced at least one APA clinically and biologically validated. In accordance with the definition proposed by the international consensus, latent porphyria refers to asymptomatic carriers of an *HMBS* deleterious variant who never experienced an APA.¹⁹ Thirty independent samples were collected in the latent porphyria (LP) group and 84 in patient with overt disease, including 64 outside of an APA (i.e., after a minimum of 3 weeks following the APA; hereafter designated as OD) and 20 during an APA but before any treatment (APA group). To clearly distinguish phenotypes we choose to compare LP (defined by a PBG level above or equal at 4 $\mu\text{mol}/\text{mmol}$ Cr by the international consensus) to an OD group including exclusively patients with a residual PBG level above 10 $\mu\text{mol}/\text{mmol}$ Cr between APAs. Thus we excluded intermediary phenotypes such asymptomatic high excretor, or asymptomatic acute porphyria (according to the new nomenclature). Finally we compared patients into LP, which had metabolically inactive disease, and OD, which retained metabolic dysfunction between crises. Samples from the LP and OD groups were all collected from different patients. Ten patients has been sampled during an attack (included in APA) and between attack (included in OD).

To refine the study, OD was divided into two subgroups with a mild phenotype ($n = 46$, designated hereafter mOD, with less than one APA per year during the last 5 years), and OD with a severe phenotype ($n = 18$, “sOD” with at least one APA per year) (Table S1). This subdivision allowed us to obtain well-balanced groups for statistical analysis. Table S2 reports the demographic and biological characteristics of each group. Patients were recruited according to the sex ratio of the groups. As the penetrance of AIP is nearly maximal at age 40, 90% of the patients recruited in LP are older than 40 years. The average ages of patients in LP and mOD were similar, and those in sOD were younger.

Based on the results of the untargeted study, targeted profiling of bile acids (BA) was conducted using a second cohort of samples. BA profile analysis, which is more relevant in blood, was performed in 74 blood samples matching (sex and age) with the untargeted study groups (20 patients in LP, 20 patients in mOD, 16 patients in sOD and 18 patients in an additional treated OD group). Urine BA profiling was also performed on a representative sample of the first urine cohort used for the untargeted approach (Figure 1). BA targeted analysis was completed with an additional group (18 blood and 10 urine samples) of severe patients treated with givosiran (Givlaari®; Alnylam Pharmaceuticals, Cambridge, MA, USA), called gOD (Figure 1 and Table S3). Blood was collected as part of routine care with a clot activator

to obtain serum. In gOD, treatment started at least 6 months before the first sampling. All the patients in gOD exhibited a very severe phenotype before treatment initiation.

2.2 | Untargeted metabolomics using liquid chromatography coupled to high-resolution mass spectrometry

Prior to analysis, the urine samples were standardized to the specific gravity by dilution to adjust to the same optical density (1.045). Then, the samples were diluted 1/3 in the mobile phase before injection into the liquid chromatography coupled to high-resolution mass spectrometry (LC–HRMS) system. The quality control (QC) samples were prepared by mixing 20 μ L of each extracted sample. QC samples were injected every five samples.

The analytical conditions were previously described²⁰ and are summarized in Appendix S1. Briefly, untargeted metabolomics experiments were performed by LC–HRMS using a combination of two complementary chromatographic methods, namely, reversed-phase chromatography (C18 chromatographic column) and hydrophilic interaction chromatography (HILIC), for the analysis of hydrophobic and polar metabolites, respectively. LC–HRMS experiments were conducted on an Ultimate 3000 chromatographic system (Thermo Fisher Scientific) coupled to Exactive/Q Exactive high-resolution mass spectrometers from Thermo Fisher equipped with an electrospray ionization (ESI) source and operating in the positive- and negative-ion modes for C18 and HILIC separations, respectively (designated hereafter as C18(+) and HILIC(–), respectively).

2.3 | Data processing and metabolite annotation

The data were processed on the Workflow4Metabolomics (W4M) platform (workflow4metabolomics.usegalaxy.fr) (Figure S1).^{21,22} In particular, automatic peak detection, integration and alignment rely on XCMS algorithms to construct a data matrix of feature intensities (areas associated with retention times RT and m/z).²³ Then, the data were filtered based on the chromatographic peak area ratio of biological to blank samples (>3), the coefficient of variation of metabolic features in QC samples ($<30\%$) and the correlation between chromatographic peak areas and QC dilution factors (>0.7). Annotation of metabolite features was first performed using our spectral database (comprising more than 1000 metabolites) according to accurately measured masses and chromatographic retention times

(RTs).²⁰ The retention time tolerances were ± 15 s and 90 s for the C18(+) and HILIC(–) modes, respectively.

After statistical analysis (described in Section 2.5), the quantification and annotation of each metabolite of interest were confirmed as follows: chromatographic peaks were integrated manually in all biological and QC samples using TraceFinder software (Thermo Fisher Scientific, Courtaboeuf, France) (Figure S1). Confirmation of metabolite annotation was then accomplished by LC–MS/MS experiments using a Dionex Ultimate chromatographic system combined with a Q Exactive mass spectrometer (Thermo Fisher Scientific) operated under nonresonant collision-induced dissociation conditions using higher-energy C-trap dissociation. Metabolite identification was based on the matching of at least two orthogonal criteria among accurate measured mass (m/z), retention time and MS/MS spectrum) to those of an authentic chemical standard analyzed under the same analytical conditions, as proposed by the Metabolomics Standards Initiative.²⁴ The statistical analyses were then rerun on these checked integrations to obtain the final results (Figure S1).

2.4 | Bile acid profiling

Bile acids (BAs) in the serum and urine of patients were analyzed using high-performance liquid chromatography coupled to tandem mass spectrometry (HPLC–MS/MS), as previously described using a QTRAP 5500 (Sciex) and detailed in Appendix S1.²⁵

2.5 | Statistical analysis

Comparisons between biological and demographic characteristics and bile acid concentrations were performed using either a Mann–Whitney hypothesis test or a Kruskal–Wallis test associated with Dunn's multiple comparison test (depending on the number of groups to compare) or a Pearson correlation test with Prism 7 software (GraphPad Software, Inc., San Diego, CA, USA) (Figure S1).

Statistical analyses of the metabolomic data were conducted on the W4M online platform. The data were first log-transformed to obtain Gaussian-like feature distributions. Then, univariate hypothesis testing was performed by using either Student's t test or analysis of variance (ANOVA) followed by Tukey's post hoc test (depending on the number of groups to be compared). The p values were adjusted to control the false discovery rate (FDR) by using the method of Benjamini and Hochberg.²⁶ Multivariate analysis consisted of data exploration with principal component analysis (PCA), followed by machine

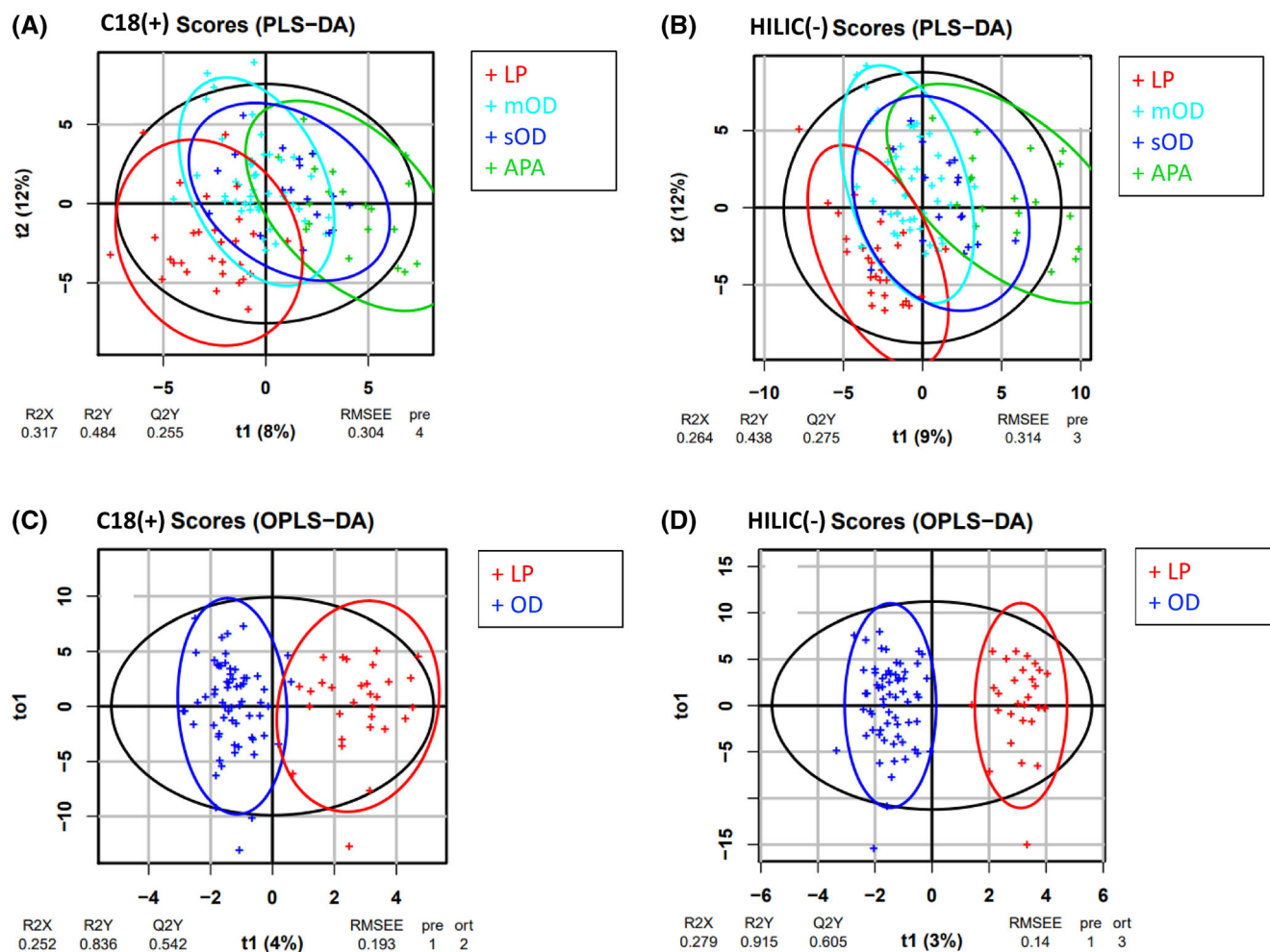


FIGURE 2 Supervised multivariate analysis of annotated features of phenotypical groups. (A, B) Comparison of four subgroups: patients with latent porphyria (LPs, red +), patients with overt disease outside of attack (OD), mild (mOD, blue sky +), severe (sOD, deep blue+) and patients during an acute attack (APA) (green +). (A) PLS-DA score plots in C18(+) acquisition mode. (B) PLS-DA score plots in HILIC(-) acquisition mode. (C, D) Comparison of patients with latent porphyria (LPs red +) with all patients with overt disease (OD: mild and severe) collected outside of an attack: Blue +. (C) OPLS-DA score plots in C18(+) acquisition mode; (D) OPLS-DA score plots in HILIC(-) acquisition mode. The 95% confidence region for each group (respectively, for all samples) is shown as a colored (respectively, black) ellipse.

learning with partial least squares-discriminant analysis (PLS-DA) and orthogonal PLS-DA (OPLS-DA).²⁷ The latter approach (OPLS-DA) facilitates interpretation (compared to PLS-DA) since OPLS-DA models contain only one predictive component in the case of a single response. The predictive variable importance in projection (VIP) from OPLS-DA models was used as the multivariate metric to rank the features. Both univariate (FDR < 0.05) and multivariate (VIP > 1.5) criteria were used to select the metabolites of interest. A metabolite set enrichment analysis (MSEA) was performed using MetaAnalyst 5.0 with the Small Molecule Pathway Database (SMPDB) as the reference.²⁸

The *biosigner* approach was used to identify a significant signatures of bile acids enabled to distinguish

between severe (sOD) and nonsevere patients (including LP and mOD group) (Figure S1).²⁹ This approach consists of selecting markers that significantly contributed to the predictive performance either with PLS-DA, a random forest, or a support vector machine classifier.

3 | RESULTS

3.1 | Untargeted metabolomics of urine samples

LC-HRMS metabolomic analysis revealed 7168 analytically relevant features (3921 in C18(+) mode and 3247 in HILIC(-) mode). Comparison with an in-house spectral

library allowed the annotation of 239 distinct metabolites (Table S4). Supervised multivariate analysis of the annotated metabolites revealed partial overlap between the different groups, suggesting phenotypic continuity between the metabolomes (Figure 2A,B). The two extreme groups, LP and APA, were clearly separated, but OD in which samples were collected outside of an APA (in either mOD or sOD) were not separated (Figure 2). Interestingly, PLS-DA performed on the whole metabolomic dataset (combining annotated and unannotated variables) provided similar results, thus showing that the set of annotated metabolites is representative of the whole dataset (Figure S2A,B).

This discrepancy in the metabolome between the samples collected during an APA and those collected between APAs (i.e., OD) was then more thoroughly investigated by univariate hypothesis testing. Eighty-eight metabolites from APA samples (data not shown) and only 16 from OD were differentially expressed compared with those in LP (Table 1). Among these metabolites, 13 overlapped in both comparisons (data not shown). Given the large number of variables which differed with the other groups, meaning that this

metabolome was strongly different, APA group was excluded from the rest of the analysis. In order to focus on understanding the metabolic conditions associated to the onset of an attack, we compared the data from the OD groups (both mOD and sOD) to those from LP using OPLS-DA and *t*-tests (Welch version for unequal variances). These analyses revealed strong differences between symptomatic and asymptomatic patients, with Q2Y values (proportion of variation explained by the model estimated by cross-validation) of 0.542 and 0.610 in the C18(+) and HILIC(-) modes, respectively (Figure 2C,D). In addition, OPLS-DA provided a predictive VIP for each annotated feature.

An ANOVA comparing pairwise the LP group with mOD and sOD highlighted five significant metabolites in C18(+) mode and nine in HILIC(-) mode (Table 1). As the post hoc tests did not reveal any significant difference between mOD and sOD, a simple *t* test comparing all the OD groups with LP was performed and revealed significant differences in four other metabolites (Table 1). Only PBG and N-acetyl-glutamine showed a significant change in both acquisition modes. All metabolites with significant variations were decreased in the OD group, except

TABLE 1 Results from univariate analysis of annotated metabolites.

Acquisition mode	Metabolites	ANOVA <i>p</i>	Post-hoc test (<i>p</i>)			<i>t</i> -Test (<i>p</i>) LP vs. OD	Fold change 10 ^{^(Δlog mean)}
			LP vs. mOD	mOD vs. sOD	sOD vs. LP		
Positive	Porphobilinogen	<10 ⁻⁴	<10 ⁻⁴	1	<10 ⁻⁴	<10 ⁻⁴	150.3
	N-acetylisoleucine	0.008	0.043	1	0.047	0.001	0.6
	Kynurenine	0.008	0.011	1	0.17	0.001	2.8
	3-Hydroxy-isovaleric acid	0.013	0.019	1	0.17	0.001	0.7
	N-acetyl-glutamine	0.034	0.106	1	0.07	0.009	0.6
	Cotinine	0.15	0.517	1	0.17	0.034	24.6
Negative	Aminolevulinic acid	<10 ⁻⁴	<10 ⁻⁴	0.387	<10 ⁻⁴	<10 ⁻⁴	3.8
	Porphobilinogen	<10 ⁻⁴	<10 ⁻⁴	1	<10 ⁻⁴	<10 ⁻⁴	520.5
	Glycodeoxycholic acid	0.001	0.001	1	0.048	<10 ⁻⁴	0.0
	Glycolic acid	0.004	0.003	1	0.141	<10 ⁻⁴	0.6
	N-acetyl-glutamine	0.02	0.189	1	0.039	0.007	0.6
	Glycocholic acid	0.005	0.05	0.853	0.026	<10 ⁻⁴	0.2
	Indolelactic acid	0.02	0.132	1	0.048	0.007	1.6
	Methyluric acid	0.025	1	0.407	0.039	0.201	0.7
	N-acetyl-phenylalanine	0.047	1	0.407	0.05	0.201	1.3
	Dihydroxybenzoic acid	0.121	0.6	1	0.141	0.041	0.4
	N-Acetyl-lysine	0.129	0.2	1	0.689	0.041	0.7
	Adipic acid	0.163	0.233	1	0.689	0.041	0.8

Note: Comparison of metabolite signals (peak areas) between patients with latent porphyria (LP) and patients with mild (mOD) and severe (sOD) overt disease (outside of attack) by ANOVA. Comparison of metabolite levels between patients with latent porphyria (LP) and patients with overt disease (OD by *t* tests). The fold change between OD and LP is expressed as 10^{^(log mean OD - log mean LP)}. Significant *p*-values are presented in bold (*p* < 0.05).

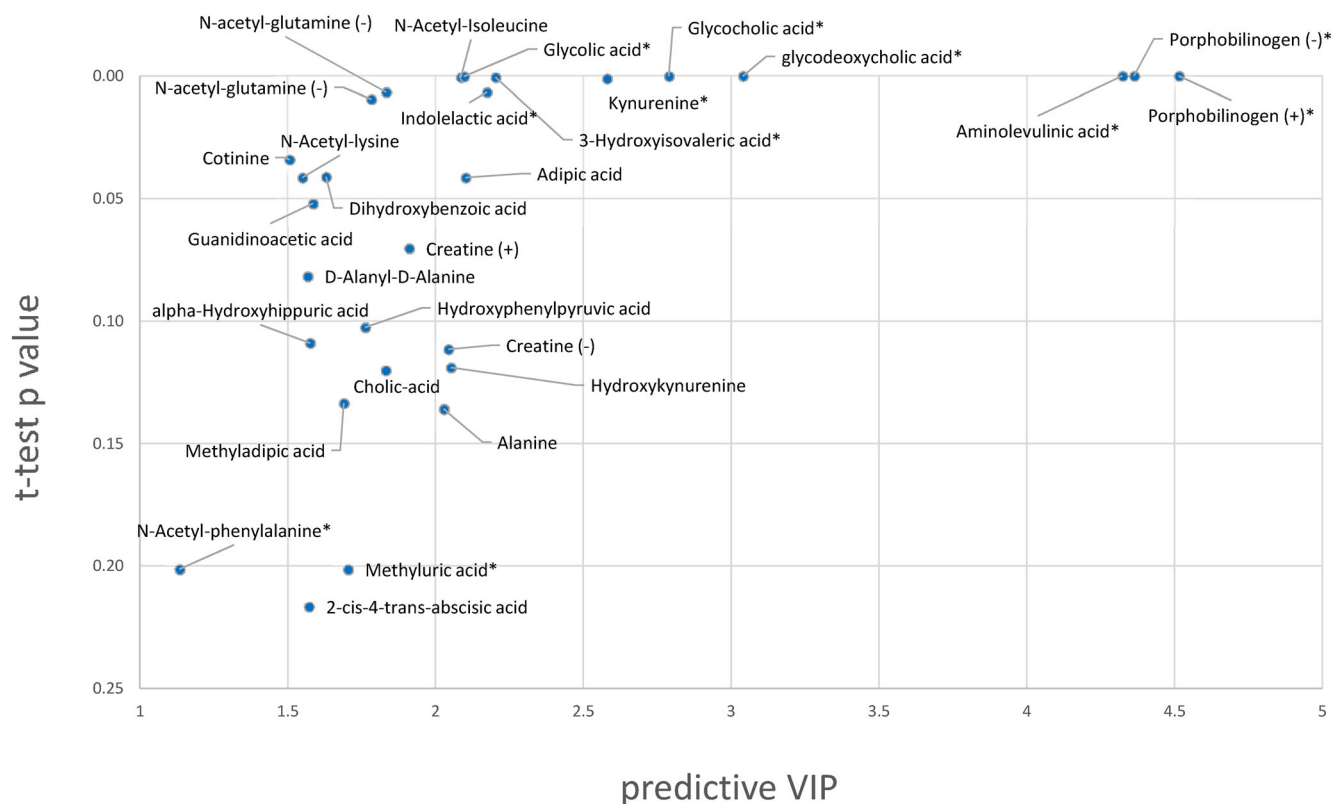


FIGURE 3 Graphical representation of features of interest resulting from untargeted analysis. Features were selected based on a maximal p value = 0.05, provided by a t test comparing asymptomatic carriers versus overt patients or a minimal predictive VIP at 1.5, provided by OPL-DA, by comparing latent porphyria (LP) and overt disease (OD). The features associated with a significant p value provided by an ANOVA, comparing the LP group and the subgroups of OD (mOD and sOD) are labeled with *. Significant features in both acquisition modes were distinguished by (+) for C18(+) and (-) for HILIC(-).

for ALA/PBG-porphyrin precursors, kynurenine, indolelactic acid, cotinine and N-acetylphenylalanine which were increased. Results of cotinine, smoker marker, confirmed the high prevalence of smokers in OD group, 48% versus 5% in LP.

By combining these relevant data with predictive VIP > 1.5 from OPLS-DA and p values < 0.05, a signature of 26 relevant metabolites in the comparison of LP group versus OD group was highlighted and is reported in Figure 3. With the highest predictive VIP and a very low p value difference compared to the second most significant metabolite, the expected AIP markers ALA and PBG allowed us to validate the overall methodology as positive controls.

Among these metabolites of interest, kynurenine, indolelactic acid and hydroxykynurenine are involved in tryptophan metabolism, and creatine, guanidinoacetic acid and glycolic acid are closely linked to glycine, the precursor of the heme pathway. Cotinine, a specific biomarker of smoking, was significantly upregulated. Unexpectedly, three bile acids, glycodeoxycholic acid, glycocholic acid and cholic acid, were also among the most relevant metabolites.

A metabolite set enrichment analysis (MSEA) allowed us to highlight the metabolic pathways most affected by the disease by taking into account the metabolic link between all the annotated features (Figure 4). As ALA and PBG levels were used as criteria for the study design, these variables were excluded from this analysis. Bile acid biosynthesis was found to be, by far, the most quantitatively and significantly altered pathway between LP and OD, with an enrichment ratio >10 and a 3-log higher p value difference compared to the second most significant metabolic pathway.

3.2 | Targeted bile acid analysis

The results from the statistical analysis comparing the metabolic profiles of LP group to those of OD groups revealed one particular metabolic pathway: bile acid (BA) biosynthesis (Table 1 and Figures 3 and 4). Hence, a complementary metabolomic analysis was conducted by specifically targeting bile acids in LP and OD groups. Therefore, another cohort involving 74 blood samples

Overview of Enriched Metabolite Sets (Top 25)

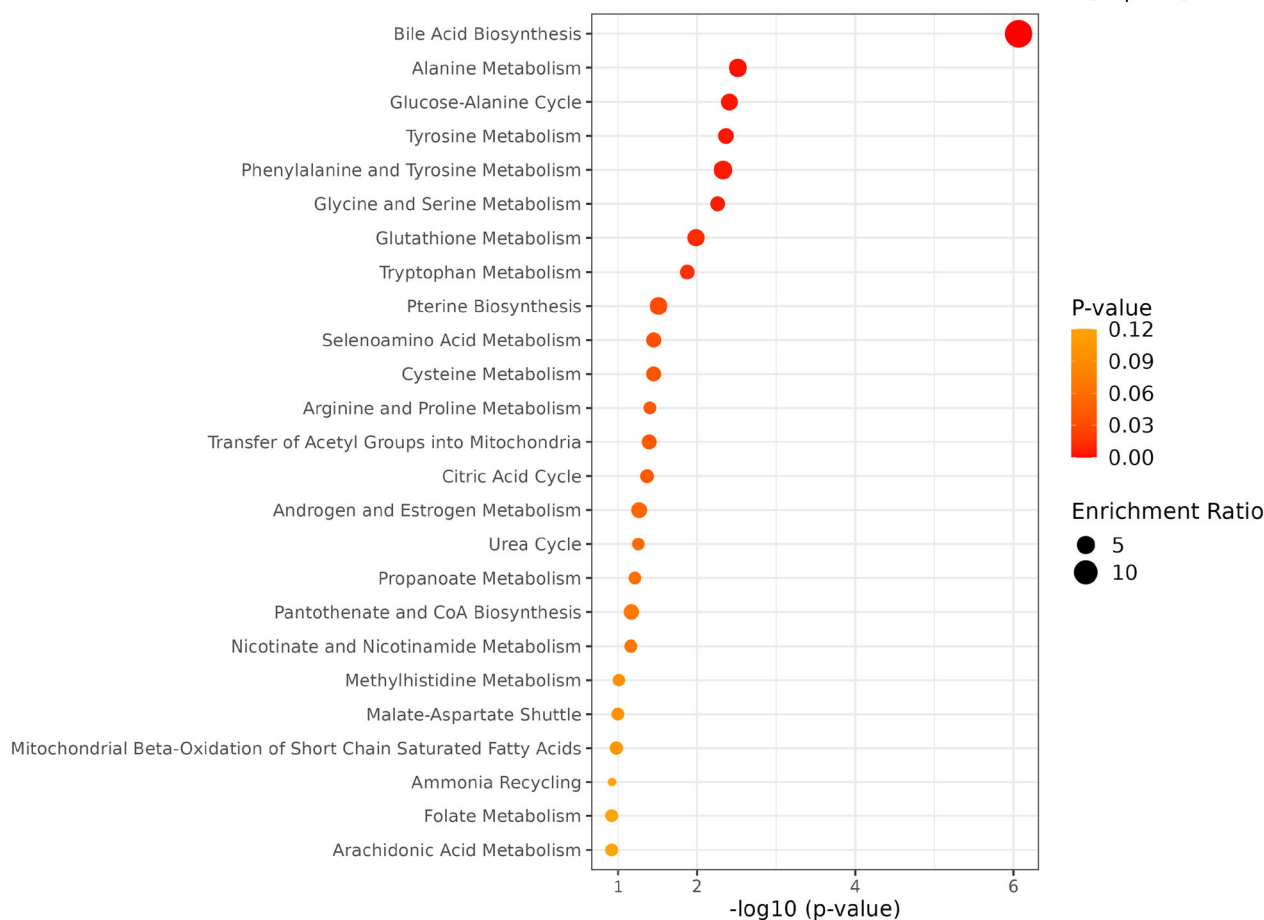


FIGURE 4 Graphical representation of a quantitative metabolite set enrichment analysis (MSEA). The data were log-transformed and mean centered. The reference library used was the Small Molecule Pathway Database (SMPDB).

was included in the second stage. The initial study design was replicated to compare the LP group with mOD and sOD groups using the same inclusion criteria and matching in terms of patient demographics and characteristics (Figure 1; Tables S2 and S3). For data comparison purposes, BAs were also quantitatively profiled in the same urine samples used for the untargeted analysis. Overall, the results obtained in urine for the three bile acids detected in the untargeted study by the semiquantitative LC–HRMS method and BA-targeted quantification showed a good correlation (Spearman $r > 0.67$) (Figure S3). Besides validating the results of the HRMS screening, those data also helped to specify the annotation of glycodeoxycholic acid, the isomer at m/z 448.306 (negative mode), which was the best correlated when comparing the two methods ($r = 0.7625$ vs. 0.2401 and 0.2821 for the other two isomeric glycochenodeoxycholic acid and glycooursodeoxycholic acid, respectively).

Although not significant, the total blood BA concentration tended to increase with disease severity

(Figure 5A). Bile acid biosynthesis comprises two parallel pathways providing two primary BAs (and consequently two secondary BAs), which can be distinguished only by the presence or absence of a hydroxyl group (OH) on carbon 12 α (Figure 5D). The HO-C12 α /non-HO-C12 α ratio in the primary BAs, the CA/CDCA ratio, decreased significantly in sOD group compared to mOD and LP groups (Figure 5B). In secondary BAs, the DCA/LCA (deoxycholic acid/lithocholic acid) ratio significantly decreased when comparing sOD to LP, and it was close to the significance threshold when comparing mOD group to LP (Figure 5C). A lower ratio strongly suggested a higher concentration of the more hydrophobic forms (CDCA and LCA) compared to the other forms. Circulating BAs are mostly conjugated, with the relative quantity of conjugated BAs increasing in mOD and sOD groups compared to that in LP patients (Figure 6A). Tauroconjugated BA concentrations were significantly greater in mOD and sOD groups than in LP, while glycoconjugated and sulfoconjugated BA concentrations were significantly greater only in the sOD group (Figure 6B–D).

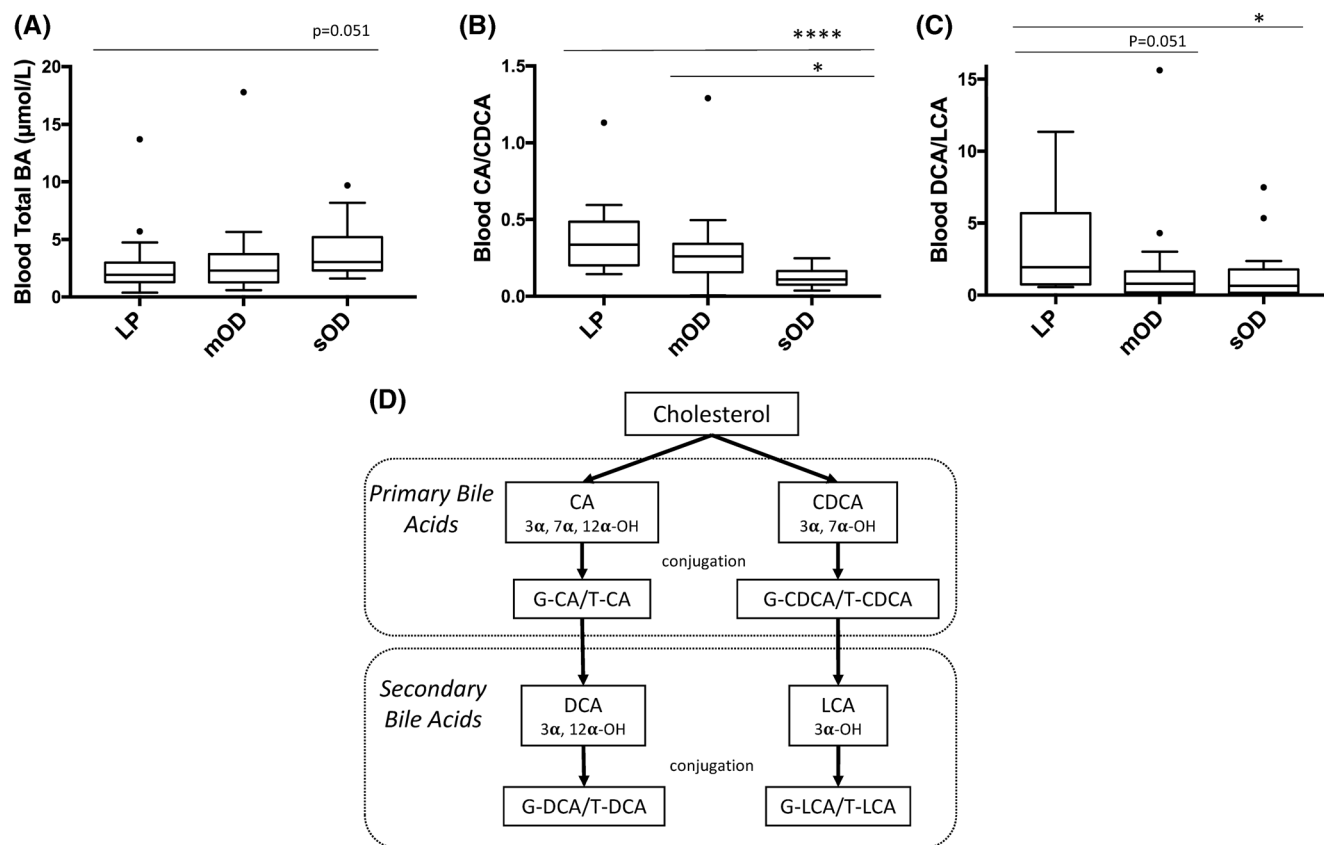


FIGURE 5 Quantitative and qualitative changes in blood bile acid levels between asymptomatic carriers and mild and severe patients. (A) Total bile acid concentrations in blood. (B) 12α -OH/non- 12α -OH ratio in blood primary bile acids (CA, cholic acid; CDCA, chenodeoxycholic acid). (C) 12α -OH/non- 12α -OH ratio in secondary bile acids (DCA, deoxycholic acid; LCA, lithocholic acid). Box plot representing the mean and 25th and 75th percentiles. The Kruskal–Wallis test and post hoc Dunn's multiple comparison test were used to compare data between groups. Significant p values are indicated by * $p < 0.05$, **** $p < 0.0001$. (D) Scheme of bile acid synthesis from cholesterol (G, glyco; T, tauro).

Tauroconjugated BAs in urine showed the same profile as those in blood. The glycoconjugation level of BAs decreased in mOD urine, but most of the urinary BAs from almost all sOD were sulfoconjugated (Figure 6E–G).

To investigate the possible direct impact of AIP pathophysiology (i.e., abnormal heme metabolism induction) on BA metabolism, we added a group of severe patients treated with givosiran (gOD). This small interfering ribonucleic acid downregulates *ALAS1*, which leads to a significant decrease in acute attacks in severe patients by repressing the first stage of the metabolic pathway.⁸ Blood BA levels were significantly greater in gOD group than in LP and mOD but not in sOD (Figure S4). As in sOD group, the HO-C12 α /non-HO-C12 α ratios were lower in gOD than in LP. Compared with LP, patients in gOD exhibit similar results than sOD, with an increase in all conjugated BAs in the blood and systematic sulfoconjugation in urine. Interestingly,

givosiran did not restore the BA concentrations within severe patients.

3.3 | CA/CDCA as a predictive biomarker of disease severity

To further identify a BA signature predicting severity, the *biosigner* recursive feature selection approach was applied between severe and non-severe patients (including LP and mOD groups). Among the set of features consisting of the BA and BA subgroup concentrations and ratios, a signature of a single variable, the CA/CDCA ratio, was repeatedly selected with the random forest classifier, providing a diagnostic accuracy of 0.84 (arithmetic mean between sensitivity and specificity) and an area under the receiving operating characteristic curve (AUROC) of 0.89 (Figure 7).

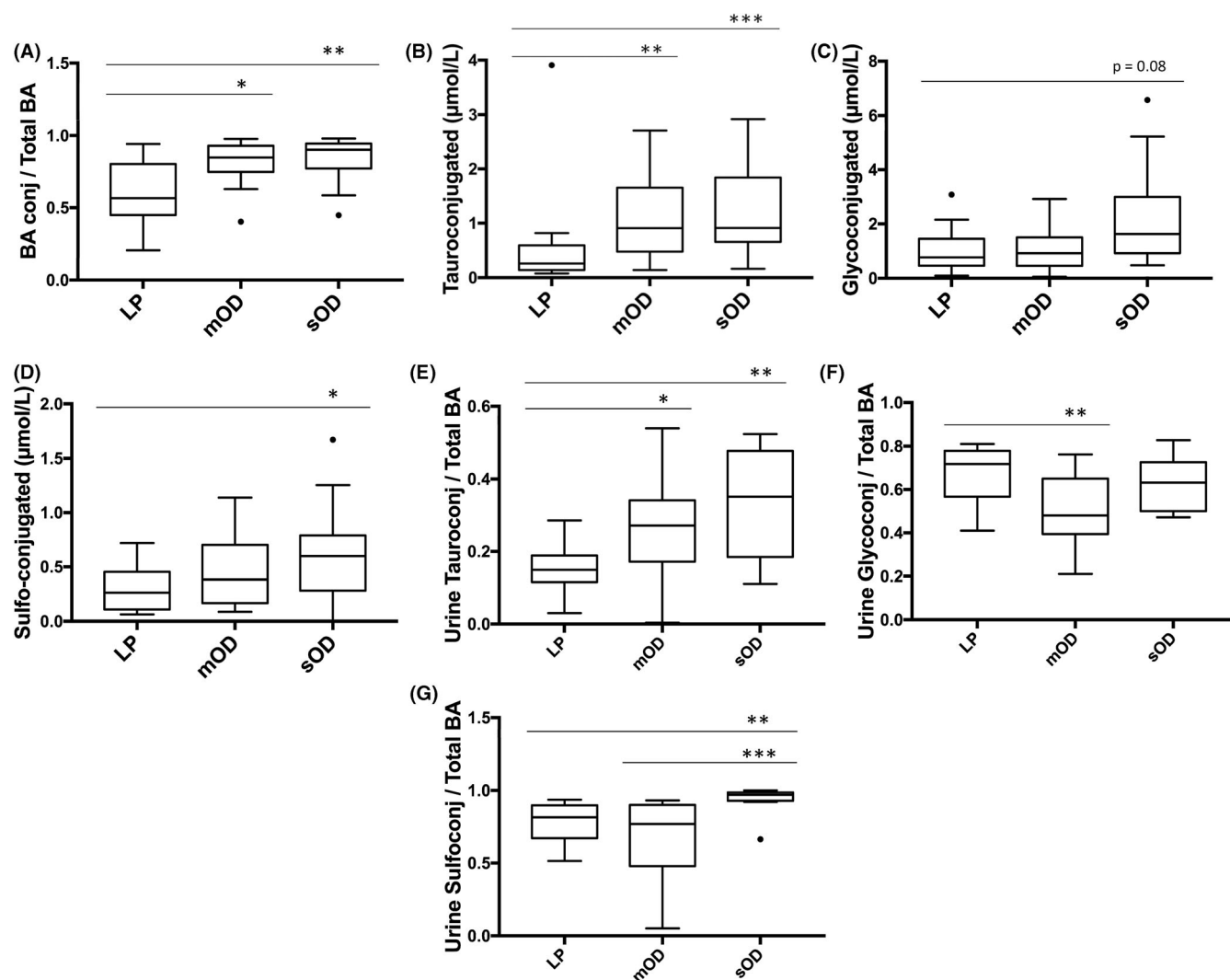


FIGURE 6 Impact of the AIP phenotype on bile acid conjugation. (A) Proportion of conjugated bile acids in blood. (B) Blood concentration of tauroconjugated bile acids. (C) Blood concentration of glycoconjugated bile acids. (D) Blood concentration of sulfoconjugated bile acids. (E) Relative concentration of tauroconjugated bile acids in the urine. (F) Relative concentration of glycoconjugated bile acids in the urine. (G) Urine relative concentration of sulfoconjugated bile acids. Box plot representing the mean and 25th and 75th percentiles. The Kruskal–Wallis test and post hoc Dunn's multiple comparison test were used to compare data between groups. Significant p values are indicated by * $p < 0.05$; ** $p < 0.01$; *** $p < 0.001$.

4 | DISCUSSION

This work reports the first untargeted urinary metabolomic study of AIP patients using high-resolution mass spectrometry. Our analytical and statistical approaches were validated, on the one hand, on the analytical side, by the high statistical significance associated with increased concentrations of the acute porphyria markers ALA and PBG in overt patients and, on the other hand, on the overall process, by the identification of metabolites belonging to the affected metabolic pathways previously described in OD group: the tryptophan pathway and glycine metabolism.^{11,13}

During episodes of neurovisceral crisis, the metabolic profile changes considerably, with 88 metabolites (on a total of 239 identified metabolites, i.e., 36%) showing significantly different concentrations during the APA compared with LP. Therefore the analysis of the APA metabolome would be too complex and beyond the scope of this study and will have to be the subject of a further dedicated study.

Significant differences in the metabolome were highlighted between asymptomatic patients and overt patients. Subgroup analysis between mOD and sOD groups revealed similar metabolomes. This finding also suggested that the metabolic mechanisms that promote

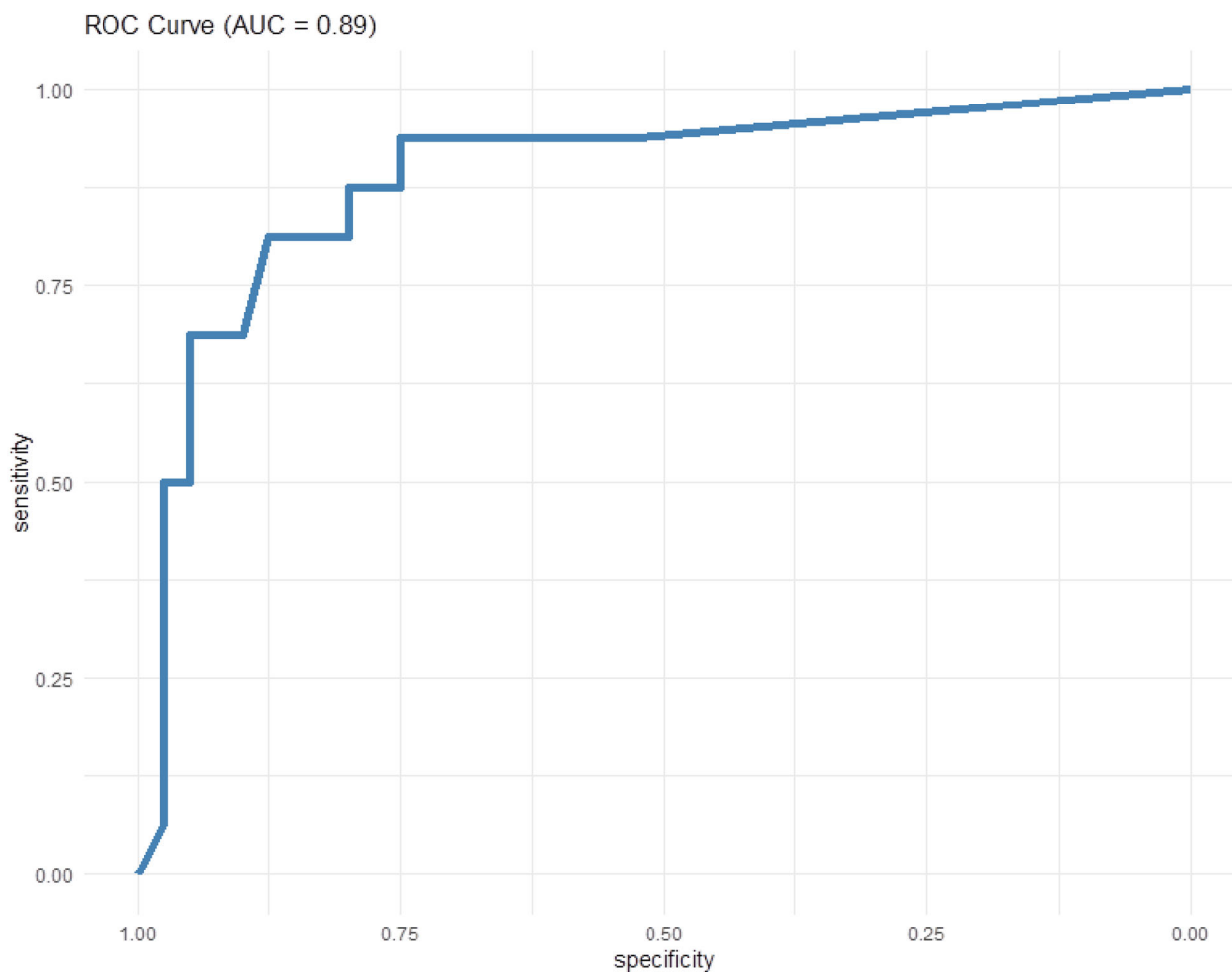


FIGURE 7 ROC curve of predictive classification in the severe group, using a random forest model trained on the CA/CDCA ratio (16 severe patients (sOD) vs. 40 nonsevere HMBS mutation carriers, i.e., LP and MOD).

these crises are similar in both groups. Thirty-eight unannotated features exhibited equivalent predictive VIPs and low p values for ALA and PBG. After excluding all adducts and in-source fragments of ALA and PBG at the same retention time, we identified approximately 30 distinct unannotated features showing similar variations than ALA and PBG (i.e., significant fold change >100 and predictive VIP > 4), which should be considered part of future structural identification work.

Our in-house chemical database covers the majority of known human metabolic pathways; thus, annotated feature analysis, including MSEA, can highlight significant changes occurring in almost all metabolic pathways. Annotated metabolite analysis did not reveal differences in metabolite concentrations higher than those observed for ALA and PBG, the reference pathological metabolites that are considered responsible for APA symptoms. However, among the annotated metabolites, several differences between asymptomatic carriers and patients with overt disease were observed and could be interpreted as

consequences of the heme metabolism disorder. Alterations in tryptophan have already been described in AIP and are thought to be the consequence of a complex mechanism combining a slight decrease in heme-dependent enzyme activity (e.g., indoleamine 2,3-dioxygenase, tryptophan 2,3-dioxygenase) and inflammation.^{11,15} The reduced concentration of metabolites related to glycine metabolism (creatine, guanidinoacetic acid or glycolic acid) in patients with overt disease, can be interpreted as a consequence of a lack of glycine availability, consumed by active heme biosynthesis. However one finding could highlight a cause of overt disease triggering. The high mean of the cotinine, a smoking marker cotinine was found in OD group, half of whom was smokers compared with 5% in LP group. This expected results suggest that patients must be advised to stop smoking.

For the first time, our study showed bile acid metabolism alterations in AIP patients. This finding was the most significant and striking results of the entire analysis.

Three BAs were identified by HRMS: cholic acid (CA), glycocholic acid (GCA) and glycodeoxycholic acid (GDCA). A targeted LC–MS/MS method subsequently confirmed these data and thus confirmed the quantitative ability of the untargeted analysis. The use of a quantitative LC–MS/MS method targeting up to 28 BAs enabled us to explore deeply BA metabolism in a comprehensive and specific manner. Interestingly, in severe patients, despite a global tendency toward an increase in BA concentration, the identified alterations consisted mainly in a change in the type of BAs. A misbalance between the two parallel pathways of BA biosynthesis, with and without HO-C12 α , underlined an increase in the proportion of hydrophobic BAs (chenodeoxycholic acid, CDCA and lithocholic acid, LCA). This abnormal characteristic was illustrated by the CA/CDCA ratio, which was identified as the most relevant marker of the clinical severity of AIP, with a high AUC (≈ 0.9), while no biological severity marker has been described for AIP until now. In addition, we found an alteration in BA conjugation associated with the degree of severity. Tauroconjugation increased in all OD groups, while glyco- and sulfoconjugation increased specifically in severe patients. Thus, mild patients exhibited a specific profile of conjugation with mostly tauroconjugation. Conjugation increases BA solubility and promotes its urinary elimination. Tauroconjugated BAs have been reported to have lower toxicity than glycoconjugated BAs.³⁰ These observations led us to hypothesize that different kinds of conjugation take part in a protection mechanism with different levels of efficacy against the accumulation of hydrophobic forms.

Bile acids can be conjugated with glycine and taurine by amidation and/or with sulfonate groups. Glycine is a precursor of heme biosynthesis. Consequently, heme pathway induction in AIP may reduce the availability of glycine.¹³ Sulfo-conjugation involves the universal sulfonate group donor 3'-phosphoadenosine 5'-phosphosulfate (PAPS), which can be provided by cysteine and taurine.³¹ Homocysteine, a sulfur-containing amino acid, is a precursor of cysteine generated by transsulfuration reactions, and a high but moderate level of homocysteine was detected in the blood of AP patients.¹⁶ Moreover, an increase in tauroconjugation associated with the activation of methionine/homocysteine metabolism leads to increased taurine, as previously reported in alcoholic liver disease.³² Thus, the availability of substrates for BA conjugation can be impacted in AIP. Other metabolic links between heme and BAs could include the targeting of the bile acid-activated nuclear receptor farnesoid X receptor (FXR) on ALAS-1 or the high preponderance of CYP-heme proteins in pathways providing different BAs from cholesterol.³³

In AIP patients, there is a greater incidence of hepatocellular carcinoma (HCC) than in the general population, which is associated with high ALA and PBG levels.³⁴ Several metabolomic analyses revealed blood bile acids as significant markers of HCC.^{35,36} A misbalance in conjugation with a greater proportion of taurine-conjugated BAs observed in our patients has already been reported at the early stage of HCC.³⁷ Thus, our findings of abnormal BA profiles in AIP patients with high levels of ALA and PBG led us to hypothesize that the dysregulation of BA conjugation plays a role in the mechanism of AIP carcinogenesis.

In AIP, the disorder consists of a partial defect of the HMBS leading to liver ALAS1 induction, as illustrated by the high concentrations of ALA and PBG in AIP patients. SiRNA-ALAS1 therapy (givosiran) efficiently reverses this pathophysiological mechanism by reducing ALA and PBG accumulation.⁸ The lack of a givosiran effect on rescuing BA metabolism allowed us to exclude a direct link between ALAS1 induction and BA disorders, and in fact, patients treated with givosiran showed a similar or even more pronounced bile acid pattern than those in sOD group. Finally, in the absence of prospective data, we cannot determine whether the bile acid profile is a consequence or cause of AIP severity.

This study has several limitations, such as the small size of the cohort, which is a common feature in studies on rare diseases. This prevents perfect age matching between the groups in our study, yet the impact on bile acids is slight as profiles vary little in adulthood. There is a continuum of phenotypes associated with AIP. It is therefore difficult to create homogeneous groups, which may reduce the power of the study. As a preliminary non-targeted metabolomics study, further works are required to validate CA/CDCA as a relevant marker of disease severity in a replicative and prospective cohort. Secondly and as mentioned above, a comparative analysis of APA metabolome with healthy subjects and inter-crisis samples from AIP patients would allow to understand pathophysiology of the attack and recurrence of APA. Indeed, healthy controls were not necessarily required in the present study which focused on the determinisms of clinical phenotype between HMBS mutation carriers. Their inclusion would allow to better understand the metabolic storm which occurs during the APA. And finally, a larger study including the excluded asymptomatic high excretors or asymptomatic acute porphyria in remission would allowed to refine the metabolome overview of AIP.

In conclusion, an untargeted LC–HRMS metabolomics approach was applied to inherited hepatic metabolic heme disorders. This analysis showed that metabolomes

differed according to whether the patient was in or out of attack, and according to the patient's phenotype (latent or overt disease). Some of the metabolic variations identified were already mentioned in literature, as tryptophan and glycine metabolism. But this study also revealed findings in an unexpected hepatic metabolic pathway. For the first time, qualitative modifications of bile acids have been described, highlighting an interaction between two important metabolites in the liver: heme and bile acids. Regardless of the origin of this BA disorder, this study provides new insights which might be involved into the pathological mechanism of HCC onset in AIP patients. Furthermore, these results open the possibility of predicting the severity of the disease and, more broadly, demonstrate the relevance of untargeted metabolomics for better delineating inherited disorders.

AUTHOR CONTRIBUTIONS

Thibaud Lefebvre: conception and design, analysis and interpretation of data, drafting the article. Thibaut Eguether: analysis and interpretation of data, drafting the article. Etienne Thévenot: conception and design, analysis and interpretation of data, drafting the article. Antoine Poli: analysis and interpretation of data, revising the article. Emeline Chu-Van: analysis and interpretation of data, revising the article. Pranvera Krasniqi: analysis and interpretation of data, revising the article. Caroline Schmitt: analysis and interpretation of data, revising the article. Neila Talbi: analysis and interpretation of data, revising the article. Gaël Nicolas: analysis and interpretation of data, revising the article. Hervé Puy: conception and design, drafting the article. Christophe Junot: conception and design, revising the article. Antonin Lamazière: conception and design, revising the article. Florence Castelli: conception and design, revising the article. Laurent Gouya: Garant, conception and design, drafting the article. François Fenaille: conception and design, drafting the article.

ACKNOWLEDGEMENTS

We would like to thank Dr. Dimitri Tchernitchko for his help in interpreting the data.

FUNDING INFORMATION

This work was supported by the funding “Poste d'accueil” of APHP.

CONFLICT OF INTEREST STATEMENT

The authors declare no conflicts of interest.

DATA AVAILABILITY STATEMENT

Data will be made available on reasonable request.

ETHICAL APPROVAL

This project was approved by the Comité d'Evaluation de l'Ethique des Projets de Recherche Biomédicale (CEERB) Paris Nord (IRB00006477) with the approval number: 2020-05. All procedures followed were in accordance with the ethical standards of the responsible committee on human experimentation (institutional and national) and with the Helsinki Declaration of 1975, as revised in 2000 (5). Informed consent was obtained from all patients for being included in the study. Proof that informed consent was obtained must be available upon request. If doubt exists whether the research was conducted in accordance with the Helsinki Declaration, the authors must explain the rationale for their approach, and demonstrate that the institutional review body explicitly approved the doubtful aspects of the study.

ORCID

Thibaud Lefebvre  <https://orcid.org/0000-0003-1398-6473>

Laurent Gouya  <https://orcid.org/0000-0002-1326-7025>

REFERENCES

- Anderson KE, Desnick RJ, Stewart MF, Ventura P, Bonkovsky HL. Acute hepatic porphyrias: “purple flags”-clinical ceatures that should prompt specific diagnostic testing. *Am J Med Sci*. 2022;363(1):1-10. doi:10.1016/j.amjms.2021.09.009
- Phillips JD. Heme biosynthesis and the porphyrias. *Mol Genet Metab*. 2019;128(3):164-177. doi:10.1016/j.ymgme.2019.04.008
- Elder G, Harper P, Badminton M, Sandberg S, Deybach JC. The incidence of inherited porphyrias in Europe. *J Inherit Metab Dis*. 2013;36(5):849-857. doi:10.1007/s10545-012-9544-4
- Lenglet H, Schmitt C, Grange T, et al. From a dominant to an oligogenic model of inheritance with environmental modifiers in acute intermittent porphyria. *Hum Mol Genet*. 2018;27(7):1164-1173. doi:10.1093/hmg/ddy030
- Chen B, Solis-Villa C, Hakenberg J, et al. Acute intermittent porphyria: predicted pathogenicity of HMBS variants indicates extremely low penetrance of the autosomal dominant disease. *Hum Mutat*. 2016;37(11):1215-1222. doi:10.1002/humu.23067
- Schmitt C, Lenglet H, Yu A, et al. Recurrent attacks of acute hepatic porphyria: major role of the chronic inflammatory response in the liver. *J Intern Med*. 2018;284(1):78-91. doi:10.1111/joim.12750
- Puy H, Gouya L, Deybach JC. Porphyrias. *Lancet*. 2010;375(9718):924-937. doi:10.1016/S0140-6736(09)61925-5
- Balwani M, Sardh E, Ventura P, et al. Phase 3 trial of RNAi therapeutic givosiran for acute intermittent porphyria. *N Engl J Med*. 2020;382(24):2289-2301. doi:10.1056/NEJMoa1913147
- Homedan C, Laafi J, Schmitt C, et al. Acute intermittent porphyria causes hepatic mitochondrial energetic failure in a mouse model. *Int J Biochem Cell Biol*. 2014;51:93-101. doi:10.1016/j.biocel.2014.03.032
- To-Figueras J, Lopez RM, Deulofeu R, Herrero C. Preliminary report: hyperhomocysteinemia in patients with acute

- intermittent porphyria. *Metabolism*. 2010;59(12):1809-1810. doi:[10.1016/j.metabol.2010.05.016](https://doi.org/10.1016/j.metabol.2010.05.016)
11. Gomez-Gomez A, Marcos J, Aguilera P, To-Figueras J, Pozo OJ. Comprehensive analysis of the tryptophan metabolome in urine of patients with acute intermittent porphyria. *J Chromatogr B Analyt Technol Biomed Life Sci*. 2017;1060:347-354. doi:[10.1016/j.jchromb.2017.06.030](https://doi.org/10.1016/j.jchromb.2017.06.030)
 12. Lelli SM, Mazzetti MB, Martín S, de Viale LC. Hepatic alteration of tryptophan metabolism in an acute porphyria model its relation with gluconeogenic blockage. *Biochem Pharmacol*. 2008;75(3):704-712. doi:[10.1016/j.bcp.2007.09.023](https://doi.org/10.1016/j.bcp.2007.09.023)
 13. Carichon M, Pallet N, Schmitt C, et al. Urinary metabolic fingerprint of acute intermittent porphyria analyzed by (1)H NMR spectroscopy. *Anal Chem*. 2014;86(4):2166-2174. doi:[10.1021/ac403837r](https://doi.org/10.1021/ac403837r)
 14. Homedan C, Schmitt C, Laafi J, et al. Mitochondrial energetic defects in muscle and brain of a Hmbs^{-/-} mouse model of acute intermittent porphyria. *Hum Mol Genet*. 2015;24(17):5015-5023. doi:[10.1093/hmg/ddv222](https://doi.org/10.1093/hmg/ddv222)
 15. Gomez-Gomez A, Aguilera P, Langohr K, et al. Evaluation of metabolic changes in acute intermittent porphyria patients by targeted metabolomics. *Int J Mol Sci*. 2022;23(6):3219. doi:[10.3390/ijms23063219](https://doi.org/10.3390/ijms23063219)
 16. Ventura P, Corradini E, Di Pierro E, et al. Hyperhomocysteinemia in patients with acute porphyrias: a potentially dangerous metabolic crossroad? *Eur J Intern Med*. 2020;79:101-107. doi:[10.1016/j.ejim.2020.04.002](https://doi.org/10.1016/j.ejim.2020.04.002)
 17. Lin CN, Shiao MS, Cheng ML, Chen CM, Kuo HC. Profiling of serum metabolites of acute intermittent porphyria and asymptomatic HMBS mutation carriers. *Cells*. 2021;10(10):2579. doi:[10.3390/cells10102579](https://doi.org/10.3390/cells10102579)
 18. Poli A, Manceau H, Nguyen AL, et al. Quantification of urine and plasma porphyrin precursors using LC-MS in acute hepatic porphyrias: improvement in routine diagnosis and in the monitoring of kidney failure patients. *Clin Chem*. 2023;69(10):1186-1196. doi:[10.1093/clinchem/hvad117](https://doi.org/10.1093/clinchem/hvad117)
 19. Stein PE, Edel Y, Mansour R, Mustafa RA, Sandberg S, Panel Members of the APE. Key terms and definitions in acute porphyrias: results of an international Delphi consensus led by the European porphyria network. *J Inherit Metab Dis*. 2023;46(4):662-674. doi:[10.1002/jimd.12612](https://doi.org/10.1002/jimd.12612)
 20. Boudah S, Olivier MF, Aros-Calt S, et al. Annotation of the human serum metabolome by coupling three liquid chromatography methods to high-resolution mass spectrometry. *J Chromatogr B Analyt Technol Biomed Life Sci*. 2014;966:34-47. doi:[10.1016/j.jchromb.2014.04.025](https://doi.org/10.1016/j.jchromb.2014.04.025)
 21. Giacomoni F, Le Corguillé G, Monsoor M, et al. Workflow4Metabolomics: a collaborative research infrastructure for computational metabolomics. *Bioinformatics*. 2015;31(9):1493-1495. doi:[10.1093/bioinformatics/btu813](https://doi.org/10.1093/bioinformatics/btu813)
 22. Guitton Y, Tremblay-Franco M, Le Corguillé G, et al. Create, run, share, publish, and reference your LC-MS, FIA-MS, GC-MS, and NMR data analysis workflows with the Workflow4Metabolomics 3.0 galaxy online infrastructure for metabolomics. *Int J Biochem Cell Biol*. 2017;93:89-101. doi:[10.1016/j.biocel.2017.07.002](https://doi.org/10.1016/j.biocel.2017.07.002)
 23. Smith CA, Want EJ, O'Maille G, Abagyan R, Siuzdak G. XCMS: processing mass spectrometry data for metabolite profiling using nonlinear peak alignment, matching, and identification. *Anal Chem*. 2006;78(3):779-787. doi:[10.1021/ac051437y](https://doi.org/10.1021/ac051437y)
 24. Sumner LW, Amberg A, Barrett D, et al. Proposed minimum reporting standards for chemical analysis chemical analysis working group (CAWG) metabolomics standards initiative (MSI). *Metabolomics*. 2007;3(3):211-221. doi:[10.1007/s11306-007-0082-2](https://doi.org/10.1007/s11306-007-0082-2)
 25. Humbert L, Maubert MA, Wolf C, et al. Bile acid profiling in human biological samples: comparison of extraction procedures and application to normal and cholestatic patients. *J Chromatogr B Analyt Technol Biomed Life Sci*. 2012;899:135-145. doi:[10.1016/j.jchromb.2012.05.015](https://doi.org/10.1016/j.jchromb.2012.05.015)
 26. Benjamini Y, Hochberg Y. Controlling the false discovery rate: a practical and powerful approach to multiple testing. *J R Stat Soc B Methodol*. 1995;57(1):289-300. doi:[10.1111/j.2517-6161.1995.tb02031.x](https://doi.org/10.1111/j.2517-6161.1995.tb02031.x)
 27. Thévenot EA, Roux A, Xu Y, Ezan E, Junot C. Analysis of the human adult urinary metabolome variations with age, body mass index, and gender by implementing a comprehensive workflow for univariate and OPLS statistical analyses. *J Proteome Res*. 2015;14(8):3322-3335. doi:[10.1021/acs.jpoteome.5b00354](https://doi.org/10.1021/acs.jpoteome.5b00354)
 28. Pang Z, Zhou G, Ewald J, et al. Using MetaboAnalyst 5.0 for LC-MS spectra processing, multi-omics integration and covariate adjustment of global metabolomics data. *Nat Protoc*. 2022;17(8):1735-1761. doi:[10.1038/s41596-022-00710-w](https://doi.org/10.1038/s41596-022-00710-w)
 29. Rinaudo P, Boudah S, Junot C, Thévenot EA. Biosigner: a new method for the discovery of significant molecular signatures from omics data. *Front Mol Biosci*. 2016;3:26. doi:[10.3389/fmolb.2016.00026](https://doi.org/10.3389/fmolb.2016.00026)
 30. Rust C, Bauchmuller K, Fickert P, Fuchsbichler A, Beuers U. Phosphatidylinositol 3-kinase-dependent signaling modulates taurochenodeoxycholic acid-induced liver injury and cholestasis in perfused rat livers. *Am J Physiol Gastrointest Liver Physiol*. 2005;289(1):G88-G94. doi:[10.1152/ajpgi.00450.2004](https://doi.org/10.1152/ajpgi.00450.2004)
 31. Klaassen CD, Boles JW. Sulfation and sulfotransferases 5: the importance of 3'-phosphoadenosine 5'-phosphosulfate (PAPS) in the regulation of sulfation. *FASEB J*. 1997;11(6):404-418. doi:[10.1096/fasebj.11.6.9194521](https://doi.org/10.1096/fasebj.11.6.9194521)
 32. Yang Z, Kusumanchi P, Ross RA, et al. Serum metabolomic profiling identifies key metabolic signatures associated with pathogenesis of alcoholic liver disease in humans. *Hepatol Commun*. 2019;3(4):542-557. doi:[10.1002/hep4.1322](https://doi.org/10.1002/hep4.1322)
 33. Peyer AK, Jung D, Beer M, et al. Regulation of human liver delta-aminolevulinic acid synthase by bile acids. *Hepatology*. 2007;46(6):1960-1970. doi:[10.1002/hep.21879](https://doi.org/10.1002/hep.21879)
 34. Lissing M, Wester A, Vassiliou D, et al. Porphyrin precursors and risk of primary liver cancer in acute intermittent porphyria: a case-control study of 188 patients. *J Inherit Metab Dis*. 2023;31:1186-1194. doi:[10.1002/jimd.12676](https://doi.org/10.1002/jimd.12676)
 35. Han J, Qin WX, Li ZL, et al. Tissue and serum metabolite profiling reveals potential biomarkers of human hepatocellular carcinoma. *Clin Chim Acta*. 2019;488:68-75. doi:[10.1016/j.cca.2018.10.039](https://doi.org/10.1016/j.cca.2018.10.039)
 36. Luo P, Yin P, Hua R, et al. A large-scale, multicenter serum metabolite biomarker identification study for the early detection of hepatocellular carcinoma. *Hepatology*. 2018;67(2):662-675. doi:[10.1002/hep.29561](https://doi.org/10.1002/hep.29561)

37. Stepien M, Lopez-Nogueroles M, Lahoz A, et al. Prediagnostic alterations in circulating bile acid profiles in the development of hepatocellular carcinoma. *Int J Cancer*. 2022;150(8):1255-1268. doi:[10.1002/ijc.33885](https://doi.org/10.1002/ijc.33885)

SUPPORTING INFORMATION

Additional supporting information can be found online in the Supporting Information section at the end of this article.

How to cite this article: Lefebvre T, Eguether T, Thévenot E, et al. Nontargeted urine metabolomic analysis of acute intermittent porphyria reveals novel interactions between bile acids and heme metabolism: New promising biomarkers for the long-term management of patients. *J Inherit Metab Dis*. 2024;1-15. doi:[10.1002/jimd.12809](https://doi.org/10.1002/jimd.12809)